

Online Research @ Cardiff

This is an Open Access document downloaded from ORCA, Cardiff University's institutional repository: <https://orca.cardiff.ac.uk/id/eprint/98210/>

This is the author's version of a work that was submitted to / accepted for publication.

Citation for final published version:

Jones, Wilm Vincent, Martin, David James, Caravaca, Angel, Beale, Andrew M., Bowker, Michael ORCID: <https://orcid.org/0000-0001-5075-1089>, Maschmeyer, Thomas, Hartley, Gareth and Masters, Anthony 2017. A comparison of photocatalytic reforming reactions of methanol and triethanolamine with Pd supported on titania and graphitic carbon nitride. Applied Catalysis B: Environmental 10.1016/j.apcatb.2017.01.042 file

Publishers page: <http://dx.doi.org/10.1016/j.apcatb.2017.01.042>
<<http://dx.doi.org/10.1016/j.apcatb.2017.01.042>>

Please note:

Changes made as a result of publishing processes such as copy-editing, formatting and page numbers may not be reflected in this version. For the definitive version of this publication, please refer to the published source. You are advised to consult the publisher's version if you wish to cite this paper.

This version is being made available in accordance with publisher policies.

See

<http://orca.cf.ac.uk/policies.html> for usage policies. Copyright and moral rights for publications made available in ORCA are retained by the copyright holders.





Contents lists available at ScienceDirect

Applied Catalysis B: Environmental

journal homepage: www.elsevier.com/locate/apcatb



A comparison of photocatalytic reforming reactions of methanol and triethanolamine with Pd supported on titania and graphitic carbon nitride

Wilm Jones^{a,b}, David James Martin^{b,c,d}, Angel Caravaca^{b,e,2}, Andrew M. Beale^{b,c}, Michael Bowker^{a,b,*}, Thomas Maschmeyer^f, Gareth Hartley^{b,f,1}, Anthony Masters^f

^a Cardiff Catalysis Institute, School of Chemistry, Cardiff University, Main Building, Park Place, Cardiff CF10 3AT, UK

^b UK Catalysis Hub, Research Complex at Harwell (RCaH), Rutherford Appleton Laboratory, Harwell, Oxon OX11 0FA, UK

^c Department of Chemistry, UCL, 20 Gordon St., London WC1H 0AJ, UK

^d FNWI, University of Amsterdam, Science Park A 904, 1073CB, Netherlands

^e School of Chemistry and Chemical Engineering, Queen's University, Belfast, UK

^f Department of Chemistry, University of Sydney, NSW 2006, Australia

ARTICLE INFO

Article history:

Received 30 September 2016

Received in revised form 12 January 2017

Accepted 16 January 2017

Available online xxx

Keywords:

Titania

Carbon nitride

Photocatalysis

Hydrogen production

Pd

Methanol

TEOA

ABSTRACT

Direct comparison between Pd supported on P25 TiO₂ and on C₃N₄ is made for photocatalytic hydrogen production, with UV activity being distinguished from visible light activity. Two very different, but commonly studied hole scavengers were used and compared, namely, methanol and triethanolamine (TEOA). Using full arc irradiation of a solar simulator the titania supported catalysts showed the best activity. Although with TEOA the carbon nitride supported catalyst shows some activity in visible light only, it is very small (ca. 15%) compared to that observed using the whole spectrum. When using methanol, even in the presence of UV light, the carbon nitride catalyst show only very low hydrogen yields.

© 2017 The Author(s). Published by Elsevier B.V. This is an open access article under the CC BY license (<http://creativecommons.org/licenses/by/4.0/>).

1. Introduction

The production of hydrogen over semiconductor photocatalysts has gained interest as an attractive method for converting solar energy into H₂ chemical energy that can be easily stored and transported [1,2]. To date, titania (TiO₂) has been perhaps the most promising and most studied semiconductor photocatalyst for hydrogen production using typical reforming reactions [3–8]. This is due largely to its abundance, non-toxicity and stability, not to mention the excellent activity under UV irradiation [9].

Typically when a semiconductor is irradiated with equal or greater energy than the band gap, photons can be absorbed to pro-

duce electron–hole (e[−] and h⁺) pairs, which can either recombine or migrate to the surface and subsequently instigate redox reactions with adsorbed species. For the case of TiO₂ the band gap is 3.2 eV (ca. 387 nm), which is in the ultra-violet region of the spectrum [10]. Since only 4% of the light incident on the Earth's surface is in the UV part of the spectrum, researchers have continually attempted to look towards harnessing visible light, which constitutes over 45% of the incident light, with a view that if semiconductor photocatalysts can harness more light overall efficiencies will be greater. Carbon nitride has recently gained interest as an inorganic semiconductor for photocatalytic water splitting that is cheap, efficient and stable [11–14]. This is predominately due to the band edge of carbon nitride 2.8 eV (ca. 450 nm) lying in the visible region of the spectrum, thus able to utilise a larger range of solar radiation compared to TiO₂. Previous studies have shown that bare TiO₂ and C₃N₄ typically demonstrate poor activity for photocatalytic hydrogen production. However, the addition of precious metal nanoparticles (NPs, e.g. Pt, Pd, Au or Ag) to the surface of the semiconductor can greatly enhance the efficiency of photocatalytic reforming reac-

* Corresponding author at: Cardiff Catalysis Institute, School of Chemistry, Cardiff University, Main Building, Park Place, Cardiff CF10 3AT, UK.

E-mail address: bowkerm@cf.ac.uk (M. Bowker).

¹ Department of Materials, Oxford University, Parks Road, Oxford, OX1 3PH, England.

² CEA, DEN, DRCP/SERA/LCAR, Bagnols-sur-Cèze, F-30207, Cedex, France.

tions [15]. This increase in activity can be understood in terms of the energy levels of the semiconductor, i.e. the photo-excited electron in the conduction band of TiO_2 can be transferred to the metal NPs. This electron can then be trapped in the NPs as result of the Schottky barrier formed, thus increasing the lifetime of the electron–hole pair and improving photoreactivity. Furthermore, the metal is also important for activation the hole scavenger molecules that are used in hydrogen production, as described earlier [2–4].

Both metal – loaded TiO_2 and C_3N_4 also demonstrate poor efficiency for photocatalytic H_2 production from pure water in the absence of scavengers. Activity is typically dramatically enhanced by the use of a hole scavenger (sacrificial agent), which injects an electron into the VB. The hole in the valence band is then filled by the electron from the scavenger, further increasing the life-time of the electron in the CB by preventing recombination and thus reduction activity. Consequently, the hydrogen produced derives partly from water splitting and partly from dehydrogenation of the hole scavenger. Common hole scavengers for a Pd- TiO_2 catalyst are simple alcohols such as methanol, ethanol and glycerol. For the case of methanol the reported products of photo-reforming are $\text{CO}_2 + \text{H}_2$, while for the case of ethanol the products have been reported as $\text{CH}_4 + \text{CO}_2 + \text{H}_2$, [16]. However, the hole scavenger almost exclusively found in relevant literature for use with a metal NP supported C_3N_4 photocatalysts is triethanolamine (TEOA).

It is rare in the literature to find the rates for these various materials and scavengers measured by the same group in the same equipment. In order to get a quantitative measure of their relative efficiency in this study we compare the photo-reforming reactions of methanol and TEOA on both Pd- TiO_2 and Pd- C_3N_4 catalysts using simulated solar light. We compare the respective activities of these materials for hydrogen evolution using methanol and TEOA as hole scavengers, deriving reaction rates in the visible and UV parts of the spectrum, in an attempt to study the different reaction mechanisms across the two photocatalysts.

2. Experimental

2.1. Catalyst preparation

Graphitic carbon nitride g- C_3N_4 was prepared by thermal decomposition of urea as reported previously [17]. The precursor urea was placed in a lidded, high form alumina crucible, then placed inside a muffle furnace and calcined in air. A ramp rate of $5^\circ\text{C}/\text{min}$ with a final temperature of 600°C held for 4 h. The resulting powder was then washed with water, HCl, NaOH and once again with water to remove all unreacted and potentially detrimental surface species. The surface area was determined by BET to be ca. $40\text{ m}^2\text{ g}^{-1}$. For reactions involving titania, Degussa/Evonik P-25 was used in all cases, which had a surface area of $52\text{ m}^2\text{ g}^{-1}$.

2.2. Incipient wetness catalysts

For the standard 0.5 wt% Pd- TiO_2 and 0.5 wt% Pd- C_3N_4 catalysts, the impregnation to incipient wetness method was used to disperse the metal on the surface of the support as described previously [18]. Briefly, a solution of PdCl_2 was prepared with the appropriate concentration of palladium required for the incipient wetness point of TiO_2 (P-25) (0.75 ml of 6.67 mg ml^{-1} Pd solution for 1 g of TiO_2 P25) and the synthesised g- C_3N_4 (6.5 ml of 0.77 mg ml^{-1} Pd solution for 1 g of C_3N_4). After thorough mixing of the solution with the TiO_2 and C_3N_4 the catalyst was dried at 200°C for two hours before calcining in air for 3 h at 400°C to produce the final state of the catalyst. Microwave plasma atomic emission spectroscopy (MP-AES) was performed on the prepared Pd- TiO_2 and Pd- C_3N_4 incipient wetness catalysts to calculate the actual Pd loading after

synthesis, details can be found in the ESI. The Pd- C_3N_4 catalyst was found to have a weight loading of 0.50% Pd as expected, and the Pd- TiO_2 catalyst was determined to contain 0.42% Pd.

2.3. In-situ photodeposition

3%Pd- C_3N_4 and 3%Pd- TiO_2 catalysts were prepared using in-situ photodeposition. Pd was deposited on the surface of the support during an induction period, whilst also simultaneously measuring the hydrogen production. Firstly, a solution of the Pd precursor, K_2PdCl_4 containing the desired mass of metal (0.6 mg) was added to the reaction mixture of water (200 ml), hole scavenger (TEOA or MeOH 0.025 mol) and support (20 mg). Secondly, this mixture was then exposed to full arc irradiation 150 W Xe lamp under reactions conditions for 3 h, with full immobilisation of the Pd assumed once the hydrogen production rate becomes stable.

2.4. Photocatalytic hydrogen production

All experiments were carried out in a 250 ml round bottom Pyrex flask equipped with a rubber septum for sample extraction using a gas-tight syringe (1 ml , Hamilton). 150 mg of the catalyst was placed in the reactor with 0.025 mol of hole scavenger and 200 ml of Milli-Q water. The initial reaction mixture was sonicated for 30 min to disperse the catalyst and provide thorough mixing of the components. The solution was then purged with argon for 30 min to remove air from the headspace and also any dissolved oxygen from the system. Illumination of the reaction mixture was performed by a 150 W Xe arc lamp (LOT-Oriel) with constant stirring using a magnetic bar. Headspace samples were taken periodically (every 30 min) by gas tight syringe and used to calculate hydrogen concentration. Analysis was performed on a Shimadzu GC (model 2014), containing Haysep-N and molsieve (Shimadzu 80–100 mesh) columns arranged in series.

The wavelength dependence of hydrogen production was determined using long pass filters (LOT-Oriel 350, 375, 400 and 420 nm) using the 0.5% Pd- TiO_2 and 0.5% Pd- C_3N_4 incipient wetness catalysts (150 mg) with TEOA as the hole scavenger (0.025 mol). After 30 min of sonication and 30 min purging with argon, each reaction was initially performed in the absence of a filter. Once the rate of hydrogen production was steady (ca. 90 min) a filter would be placed between the solar simulator and reactor, starting with the lowest wavelength. Again, once the rate was steady the next lowest wavelength filter would be put in place, and so on until either no hydrogen production was measured or the final 420 nm filter was in place.

2.5. Characterisation

Samples were prepared for TEM characterisation by dispersing the catalyst powder in high purity ethanol, followed by sonication for 10 min. A drop of this suspension was then evaporated at room temperature on a holey carbon film supported by a 300 mesh copper TEM grid (Agar Scientific). Samples were then subjected to bright field diffraction contrast imaging in order to determine particle size distribution. The TEM instrument used for this analysis was a JEOL-2100 with a LaB6 filament operated at 200 kV .

UV-vis spectra were recorded on a Shimadzu UV-2600 spectrometer using a pressed disc of the sample. Kubelka-Munk transformed diffuse reflectance spectra (DRS) of all samples were measured between 200 and 800 nm with BaSO_4 powder used as a reference.

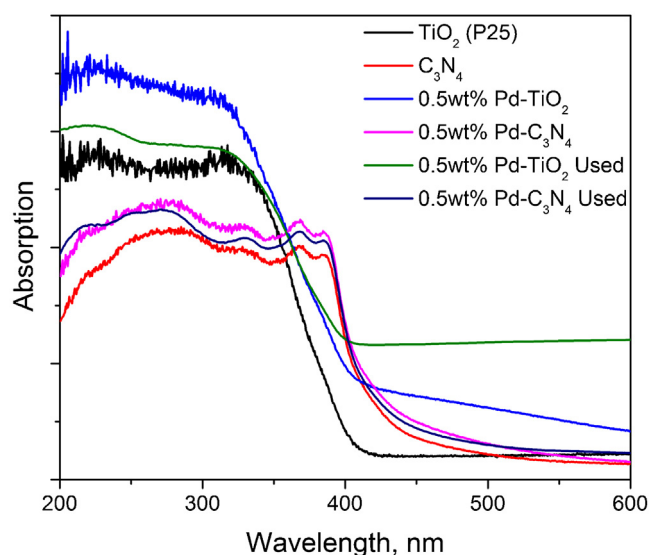


Fig. 1. UV-vis absorption spectra of pure TiO_2 (P-25) and C_3N_4 , and with 0.5% Pd loaded, both before and after use.

3. Results and discussion

3.1. UV-vis Spectra

The absorption properties of pristine TiO_2 (P-25) and C_3N_4 were analysed by diffuse reflectance UV-vis spectroscopy (Fig. 1). TiO_2 (P-25) shows negligible absorption in the visible range with a sharp increase below roughly 400 nm corresponding the band gap of TiO_2 (380 nm, 3.2 eV) [19]. In contrast, the absorption edge of C_3N_4 is shifted by roughly 20 nm towards the visible compared to TiO_2 , which can be attributed to the lower energy band gap of C_3N_4 . While the absorption edge of C_3N_4 is sharp there is a tail between approximately 440–520 nm before flattening out, this tail can be attributed to a very small amount of $n-\pi^*$ transitions [20,21].

In the region of 380 nm C_3N_4 shows transitions which can be assigned to $\pi-\pi^*$ transitions commonly observed in heterocyclic aromatics [20]. Absorption spectra of both C_3N_4 and TiO_2 prepared with 0.5 wt% Pd by incipient wetness were also recorded (Fig. 1). In both cases the shape of the absorption spectrum is broadly similar, with a slight shift in edge position to longer wavelength. However, the Pd- TiO_2 sample shows increased absorption over a broad range of wavelengths in the visible region. This is likely to be due to the presence of some residual PdO on the surface of the semiconductor remaining after the calcination step that followed the incipient wetness impregnation. This PdO can absorb visible light in the 400–550 nm range owing to the low band gap and d-d transitions of the PdO particles. [22]. After reduction the catalyst changes colour and becomes more grey, consistent with the post-reaction UV-vis, which shows increased absorption over a wide range of wavelengths. The nitride catalysts did not change colour significantly either after preparation or use.

It is worth noting that the band gap of C_3N_4 synthesised from thiourea and dicyandiamide (DCDA) have been reported to possess smaller band gaps (~ 2.75 eV) when compared to urea derived C_3N_4 . The actual value of the band gap is dictated by a variety of factors, including morphological differences, and differences in defect concentrations/stoichiometry in the lattice. However despite absorbing a little in the visible, and hence showing some visible light photocatalytic activity, Martin et al. also showed that urea synthesised C_3N_4 exhibited greater activity in photo reforming reactions under full arc illumination [14].

Table 1

Average particle size with standard deviation of Pd NPs made by in situ photodeposition for reaction of TiO_2 and C_3N_4 with MeOH and TEOA.

Catalyst system	Range of highest occurrence (nm)
3%Pd- C_3N_4 MeOH	2–5
3%Pd- C_3N_4 TEOA	2–6
3%Pd- TiO_2 MeOH	2–3
3%Pd- TiO_2 TEOA	4–7

3.2. Transmission electron microscopy

TEM analysis of both the used and unused 0.5% Pd weight loading incipient wetness catalysts was performed. However, no Pd NPs were observed in any sample. Thus, it was assumed that the Pd NPs formed by this method were too small and well dispersed to be observed. Additionally as bright field TEM creates an image by Z contrast the PdO NPs expected on the prepared catalysts would be harder to observe compared to Pd NPs due to the differences in density. Analysis of the 3 wt% Pd- C_3N_4 and 3%Pd- TiO_2 catalysts after reaction with either MeOH or TEOA was performed by TEM to gain information on the particle size and morphology of the Pd NPs produced during in-situ photo-deposition. Representative images of each along with particle size histograms are shown in Fig. 2. As can be seen, in all cases the Pd NPs are well dispersed over the surface of the support. The Pd particles photo-deposited on C_3N_4 have some heterogeneity containing agglomerates of particles, whereas the Pd particles on TiO_2 shows primarily spherical particles homogeneously dispersed with a narrow particle size distribution.

Table 1 shows the range of particle sizes of the Pd NPs, that were generated during the 3 wt% Pd- C_3N_4 and 3 wt% Pd- TiO_2 reactions with either MeOH or TEOA. Particle sizes for the Pd on C_3N_4 made from both hole scavengers differ by around 1 nm with a range of sizes of 2–6 nm for the MeOH reaction and 3–6 nm for the TEOA reaction. Whereas the particle size observed after the photo-deposition reaction on TiO_2 differs more substantially (2–3 nm for the MeOH reaction and 4–7 nm for the TEOA reaction). It is interesting to note that the range of particle sizes for Pd is smaller after reaction with MeOH for both C_3N_4 and TiO_2 even though the rate is less for this reaction than for the TEOA equivalent. It is therefore unlikely that the higher activity of the TEOA reactions is due to a particle size effect as smaller NPs have a higher metal surface area and so are typically more active. For the Pd to be reduced, photo-excited electrons in the conduction band need to be transferred to the Pd precursor in solution, whilst the hole in the valence band will need to be reduced by the hole scavenger. As the role of TEOA and MeOH in these reactions is to remove the hole then the efficiency of this process could affect the particle size during the photo-deposition.

4. Photocatalytic performance across the full simulated solar spectrum

4.1. Incipient wetness impregnation catalysts

Fig. 3 shows hydrogen production from both methanol and TEOA for 0.5% Pd- C_3N_4 and 0.5% Pd- TiO_2 made by the incipient wetness method. Both reactions were run under identical conditions (150 mg of catalyst in 200 ml of 0.125 M solution of hole scavenger) using a 150W Xe arc lamp solar simulator with no filters in place. As can be seen the choice of hole scavenger and semiconductor has a strong influence on the quantities of hydrogen produced. Both reaction systems follow the same trend, with TEOA producing a greater yield of hydrogen compared to methanol. The titania based catalysts were significantly more active with full arc illumination than those of C_3N_4 , titania producing of the order of 8 times

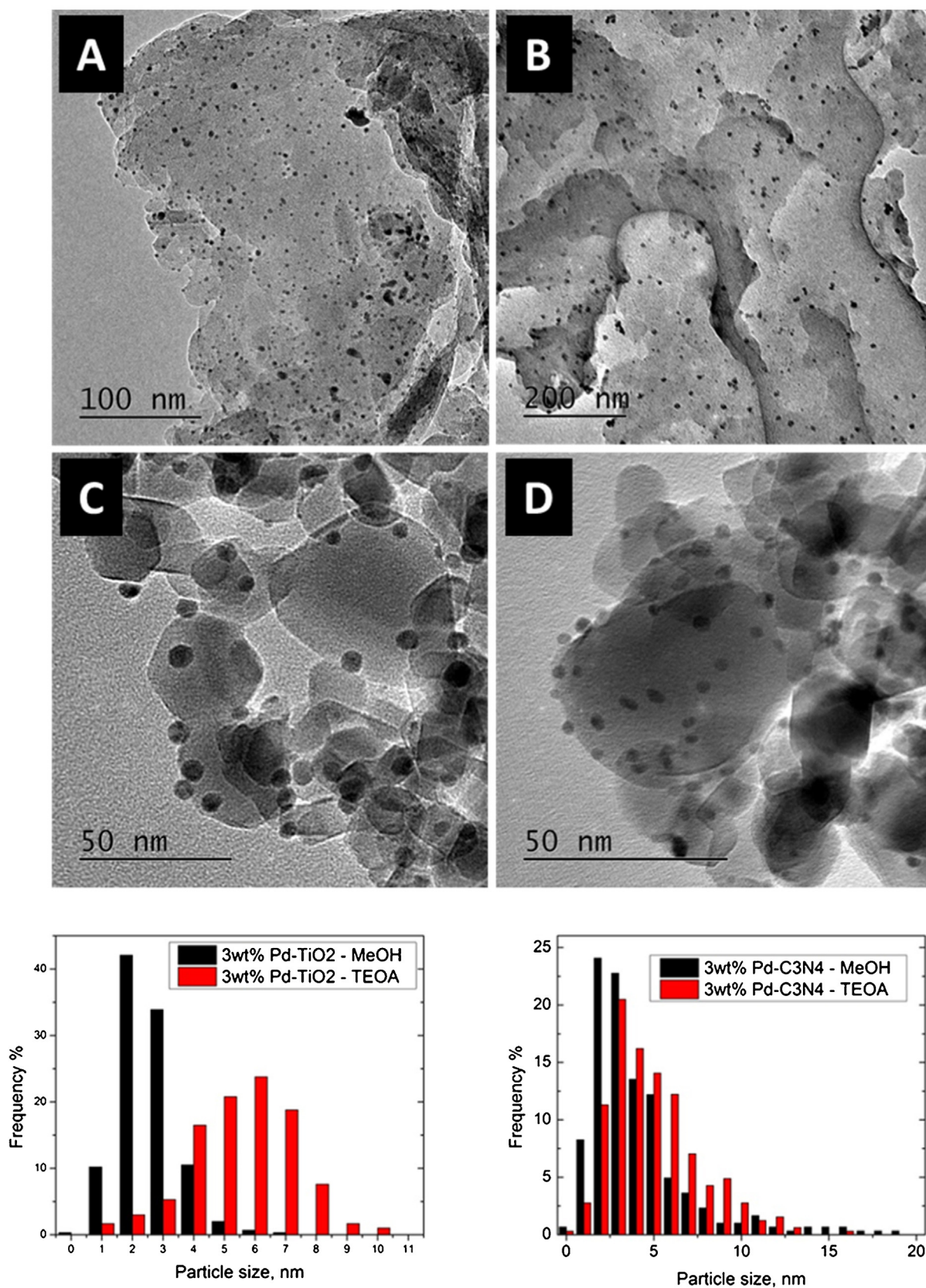


Fig. 2. TEM images of 3% Pd-C₃N₄ after reaction with A) MeOH B) TEOA and 3% Pd-TiO₂ after reaction with C) TEOA and D) MeOH. The particle size histograms are also shown, obtained from counts of more than 300 nanoparticles.

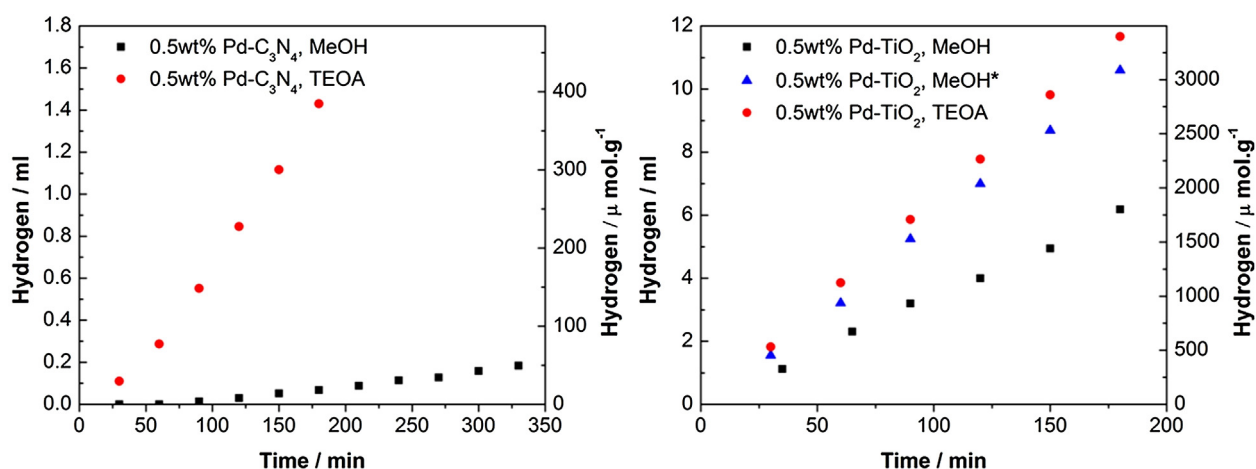


Fig. 3. Hydrogen production plots for reactions with 150 mg catalyst, *0.09 mol of methanol used. The left axis displays the hydrogen evolved in ml, while on the right data is given as $\mu\text{mol g}^{-1}$.

more hydrogen for the TEOA reactions and 60 times more hydrogen for the methanol reactions after 3 h. Although the concentrations of the hole scavengers are identical, methanol contains only four hydrogen atoms while TEOA has 15 and thus this could be one contribution to the improved hydrogen yield for TEOA for the Pd/TiO₂ sample. Thus, in Fig. 3 we also show the hydrogen evolution comparison for TEOA and methanol when the same number of moles of hydrogen are present in the sacrificial agent, and then the hydrogen evolution is very similar for the two.

For the case of the Pd – C₃N₄ sample, it is of particular note that the yield of hydrogen from aqueous methanol was significantly less than that of TEOA, especially when compared to the Pd-TiO₂ catalyst, while the latter shows little difference between the two hole scavengers. Also an induction period of about 90 min was seen before hydrogen was evolved for the methanol reaction, whereas with TEOA hydrogen production began immediately.

This difference can be explained when considering the necessity for the metal to be in the reduced, metallic state, as a prerequisite for the reaction to produce hydrogen. The Pd begins in the oxidic state, since it was calcined in air prior to use, and is photoreduced during the reaction. Actual, hydrogen evolution begins only once the Pd is fully reduced. Indeed, at least 0.08 ml of hydrogen would be needed to reduce the 4 μmol of PdO present. At the rate of hydrogen evolution observed for the methanol reaction on Pd/C₃N₄ (after 90 mins it is ca. 7×10^{-4} ml/min) that would take around 100 min, as observed. On the other hand, on Pd/TiO₂, the rate is 3×10^{-2} ml/min, which corresponds with only around 3 min for reduction, which is before the first data point is measured. However, it is usually our contention that it is necessary to have the nanoparticles in the metallic form to be active. This then, appears only to be the case in the sense that before the metal is reduced the hydrogen which could be produced is used up in reducing the oxide to metal. As we showed recently⁶ the ability to produce hydrogen depends on the reducibility of the metal, so Ni, for instance, will not produce hydrogen normally, but will if it is carefully pre-reduced before placing in the photoreactor. The implication of these findings could be that the transfer of a photo-activated hole from the titania to the nanoparticle oxide adsorbed on it actually limits the initial reduction process.

The lower reaction rate and the induction time for methanol indicates that it is a poor hole scavenger for C₃N₄. In contrast, TEOA is obviously a much better scavenger – yet it works even better with TiO₂. The poor behaviour for methanol on the nitride is explained by the mechanism we have previously proposed for the reaction on Pd-

TiO₂ [2,16] which we describe as the photo-reforming of methanol. Basically it can be summarised as follows –



Here step 1 proceeds on the Pd nanoparticles, since methanol has been shown to decarbonylate at ambient temperature [4,16,23] and leaves CO adsorbed on the surface. When the surface is saturated with CO, no further reaction takes place (self-poisoning) until step 2 occurs by bandgap excitation in the TiO₂ to create an electron-hole pair. The CO is then cleaned off the Pd by the highly electrophilic oxygen species (the hole) in step 3. The final step is filling of the vacancy (V₀) in the titania by water. Thus, an essential element of this scheme is the active surface oxygen and this is not available on carbon nitrides surface, hence the very low reaction rate on that material.

This then raises questions regarding the mechanism of reaction of TEOA. Since this does react on the nitride significantly, it is likely that reaction proceeds through the nitrogen group, initially presumably via the lone pair of the nitrogen. Indeed, work in progress in the group and elsewhere [24,25] shows that amines react well photocatalytically with both materials. We know little about the mechanism of this part of this reaction, except that it is a net dehydrogenation. When comparing the two semiconductors with these identical reaction parameters, using the full spectrum of simulated solar light, it is clear that titania is significantly more active for photocatalytic hydrogen production with TEOA and methanol.

A second set of comparison reactions under different reaction parameters was also performed, using a much lower amount of 20 mg of the semiconductor (20 mg) in 200 ml of 0.125 M solution of hole scavenger with 3 wt% Pd loading. This was because reaction parameters for photocatalytic reactions involving carbon nitride can vary in the literature, however it is perhaps most common to use a relatively small amount of the catalyst (5–50 mg) with higher loadings of metal compared to reactions involving TiO₂. [17,26]. The results are basically very similar to those already described, and are presented in the supplementary material.

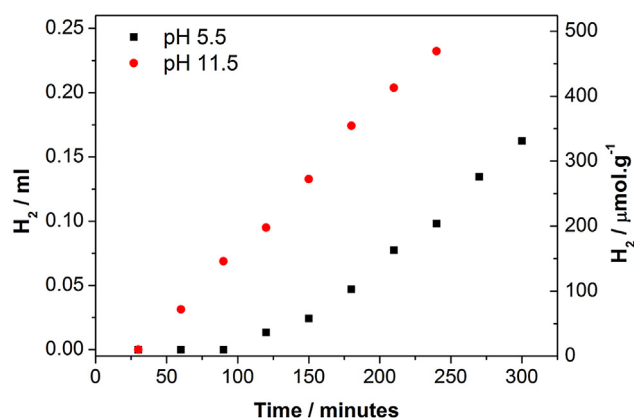


Fig. 4. Hydrogen production plots for reactions with 20 mg catalyst 3% Pd- C_3N_4 0.025 mol of methanol at pH 5.5 and 11.5 adjusted with NaOH. The left axis displays the hydrogen evolved in ml, while on the right data is given as $\mu\text{mol.g}^{-1}$.

4.2. Photo-deposition catalysts

In-situ photo-deposition by irradiation with UV light is a common method for reducing metal precursors to prepare NPs immobilised onto semiconductor surfaces. It has been reported that the role of the semiconductor such as TiO_2 or C_3N_4 , during photo-excitation is to transfer electrons from the valence band to the metal precursor, whilst the hole reacts with a scavenger species. [27,28] This results in the formation of Pd NPs in a dispersed manner across the surface of the C_3N_4 , as can be seen in the TEM images in Fig. 2, (discussed in more detail below).

The hydrogen evolution plots of the second set of comparison reactions with the Pd deposited by in-situ photo-deposition are shown in Fig. S1. Similar to the results for the incipient wetness method, TEOA was again found to be the most active hole scavenger for such materials with the titania based catalysts being the most active. The higher yield of hydrogen from TEOA is explained by the increased hydrogen content and extra functional groups of the molecule compared to methanol, as shown in Fig. 3. However, a rate of hydrogen production from TEOA that is much higher than that of MeOH cannot be explained solely by the extra OH groups of TEOA. Therefore, it may be that the nitrogen functional group on TEOA is responsible for the majority of the activity observed, and is primarily responsible for the rapid deposition of the Pd.

It is worth noting that the pH of the initial reaction mixture containing TEOA, carbon nitride and water is very basic (pH 11.5 for 0.025 mol in 200 ml milliQ water) while the reaction mixture containing MeOH, carbon nitride and water was slightly acidic (pH 5.5 for 0.025 mol in 200 ml milliQ water). To investigate this further a reaction was preformed where NaOH was added to carbon nitride methanol mixture before the reaction to adjust the pH to 11.5. Fig. 4 shows the hydrogen production plots for the 3 wt% Pd *in situ* photodeposition reactions of g- C_3N_4 with methanol at pH 5.5 and 11.5. The rate measured with the pH 5.5 and 11.5 reactions was 9.28×10^{-4} and $11.3 \times 10^{-4} \text{ ml min}^{-1}$ of H_2 respectively. This corresponds to an improvement in rate of about 22% for the reaction at higher pH, once the rate becomes stable. This is likely to be another factor as to why the MeOH reaction on Pd- C_3N_4 produced less H_2 than the TEOA reaction. However it is thought that the arguments made in previous sections are still valid as the changes observed in the rate are small compared to the large increase in rate of TEOA over MeOH measured.

Wu et al. found a positive effect of high pH on visible light driven hydrogen evolution reactions of Pt loaded g- C_3N_4 from a 20% vol methanol solution. Although it wasn't until pH \gg 10 that a significant change in H_2 production rate was observed. [29] The reaction

parameters used by Wu et al. varied to what was used in this study, i.e. 20% vol methanol solution, 1 wt%Pt as the metal co-catalyst and a 400 nm long band pass filter. This could be a factor as to why we did not see as much of an improvement in rate at higher pH for the methanol reaction. Wu et al. suggested the increased activity is due to an increase in driving force for photochemical methanol oxidation at high pH. If this is correct it could be a factor as to why the induction period for the reaction at higher pH was reduced by about \sim 90 min in our measurements.

5. Photocatalytic performance under simulated visible light

As shown in the UV-vis spectra (Fig. 1), C_3N_4 absorbs light in the visible range compared to the TiO_2 . The band gap of the urea synthesised C_3N_4 is estimated to be in the region of 420 nm (2.9 eV) while that of P-25 titania is 387 nm (3.2 eV). Hence we might anticipate enhanced activity of these materials due to this extra visible absorption.

To investigate the wavelength dependence of photocatalytic activity, long band pass filters (350, 375, 400 and 420 nm) were used to block the UV region of the incident irradiation during the photocatalytic reactions of C_3N_4 and TiO_2 . Fig. 5 shows the average rate of hydrogen production from incipient wetness 0.5% Pd- TiO_2 and 0.5% Pd- C_3N_4 catalysts using TEOA as the hole scavenger. As might be expected for the 0.5%Pd- TiO_2 catalyst, the rate of hydrogen production decreases as the UV region is blocked until no hydrogen is produced with the 400 nm filter in place, which is consistent with the TiO_2 band gap of ca. 390 nm. Note that the UV-vis spectra of 0.5% Pd- TiO_2 show significant absorption in the visible region, but this does not contribute at all to any photocatalytic activity. For the 0.5%Pd- C_3N_4 catalyst system, again the rate of hydrogen production decreases with successive addition of the long band pass filters of 350, 375 and 400 nm, but does have some activity for the 400 nm filter, that is, in the visible. This is consistent with the UV-vis spectrum of the carbon nitride support. However, when a 420 nm high band pass filter was employed neither the C_3N_4 nor the TiO_2 catalyst produced any hydrogen after 3 h of illumination. So some visible light activity is observed for the nitride supported catalysts, but it is very low and much lower than when full spectrum light is used.

It must be noted that carbon nitride exists in a number of forms and stoichiometry, and these variations can have some effect on activity. In particular, Li et al [30] have recently shown that pre-hydrogenation of the nitride can result in an enhancement in activity in the visible of a factor of six or so.

6. Conclusions

Comparison of graphitic carbon nitride and P-25 titania, both loaded with Pd has been made for photocatalytic hydrogen production from TEOA and MeOH. When irradiated with a solar simulator, Pd/P25 titania was found to be the most active for these reactions. Of the hole scavengers used TEOA was demonstrated to be more active for this reaction compared to MeOH and Pd/ C_3N_4 showed almost no activity for methanol photo-reforming. Photocatalytic hydrogen production using graphitic carbon nitride is shown to be strongly correlating with the hole scavenger used; TEOA is over 14 times more effective than methanol. However under the same conditions but using TiO_2 , it was demonstrated that TEOA is only twice as effective at scavenging holes in comparison to methanol. By performing tests under identical pH conditions, we experimentally verified that the pH difference between TEOA and methanol in aqueous solutions is not the reason for enhanced activity, with the presence of a nitrogen group thought to be more significant.

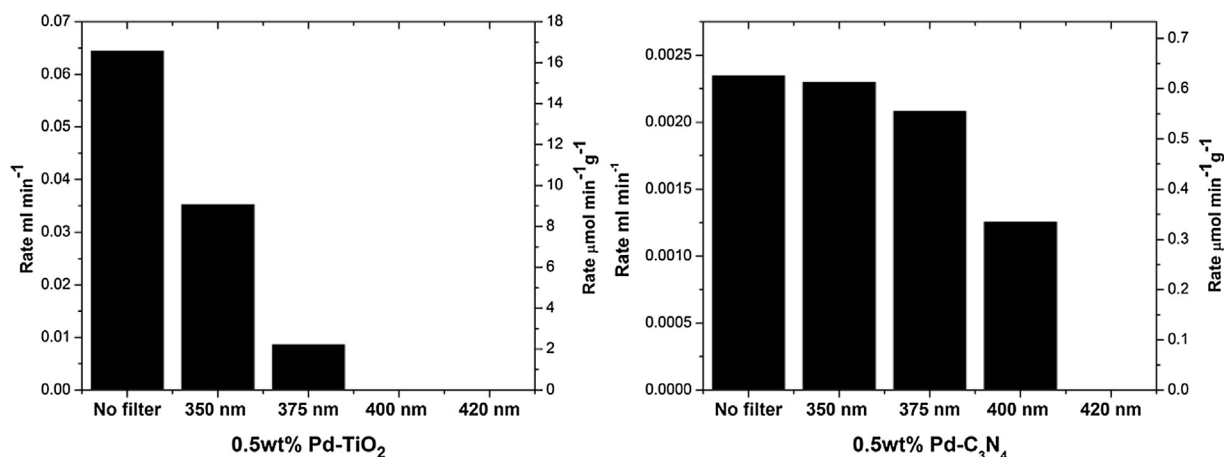


Fig. 5. Average rates in ml min^{-1} and $\mu\text{mol min}^{-1}$ of hydrogen production with a set long band pass filters (350, 375, 400 and 420 nm) for left, 0.5%Pd-TiO₂ and right, 0.5%Pd-C₃N₄ with TEOA reaction. The left axis displays the hydrogen evolved in ml min^{-1} , while on the right data is given as $\mu\text{mol min}^{-1} \text{g}^{-1}$.

Photocatalytic tests were performed with long band pass filter in place to block out the UV radiation, allowing only visible light to interact with the TiO₂ and g-C₃N₄ based catalysts. Under these conditions g-C₃N₄ based catalysts were found to be active partially into the visible, with wavelength above 400 nm, but not above 420 nm. The equivalent reaction using TiO₂ based catalyst was found to be inactive for visible light, but significantly more active with UV irradiation than the g-C₃N₄ based catalysts. This leads to the conclusion that g-C₃N₄ based catalysts have the advantage over TiO₂ based catalyst in that activity is observed with longer wavelength of light. However the rates of hydrogen production are poor, especially when under to full arc conditions for both semiconductors. Therefore currently pure undoped g-C₃N₄ based photocatalysts are inferior to TiO₂ based catalysts.

Acknowledgements

The authors are grateful for support for this work through the award of an International Research Collaboration Award from Sydney University to MB, and research funds from EPSRC through grants EP/K014854/1, EP/K014714/1 and the EC through H2020 Spire grant MefCO2 reference number 637016. We would also like to thank June Callison for performing MP-AES measurements.

Appendix A. Supplementary data

Supplementary data associated with this article can be found, in the online version, at <http://dx.doi.org/10.1016/j.apcatb.2017.01.042>.

References

- [1] C.G. Silva, R. Juarez, T. Marino, R. Molinari, H. Garcia, J. Am. Chem. Soc. 133 (2011) 595–602.
- [2] M. Bowker, C. Morton, J. Kennedy, H. Bahruji, J. Greaves, W. Jones, P.R. Davies, C. Brookes, P.P. Wells, N. Dimitratos, J. Catal. 310 (2014) 10–15.
- [3] M. Mrowetz, A. Villa, L. Prati, E. Selli, Gold Bull. 40 (2007) 154–160.
- [4] L.S. Al-Mazroai, M. Bowker, P. Davies, A. Dickinson, J. Greaves, D. James, L. Millard, Catal. Today 122 (2007) 46–50.
- [5] A. Fujishima, X.T. Zhang, D.A. Tryk, Surf. Sci. Rep. 63 (2008) 515–582.
- [6] H. Bahruji, M. Bowker, P.R. Davies, J. Kennedy, D.J. Morgan, Int. J. Hydrogen Energy 40 (2015) 1465–1471.
- [7] M. Bowker, L. Millard, J. Greaves, D. James, J. Soares, Gold Bull. (2004), <http://dx.doi.org/10.1007/bf03215209>.
- [8] P. Claus, A. Brückner, C. Mohr, H. Hofmeister, J. Am. Chem. Soc. 122 (2000) 11430–11439.
- [9] M.D. Hernandez-Alonso, F. Fresno, S. Suarez, J.M. Coronado, Energy Environ. Sci. 2 (2009) 1231–1257.
- [10] K.M. Reddy, S.V. Manorama, A.R. Reddy, Mater. Chem. Phys. 78 (2003) 239–245.
- [11] M.S. Chen, D.W. Goodman, Science (2004).
- [12] A.A. Herzing, C.J. Kiely, A.F. Carley, P. Landon, G.J. Hutchings, Science 321 (2008) 1331–1335.
- [13] N. Dimitratos, J.A. Lopez-Sanchez, D. Morgan, A.F. Carley, R. Tiruvalam, C.J. Kiely, D. Bethell, G.J. Hutchings, Phys. Chem. Chem. Phys. 11 (2009) 5142–5153.
- [14] D.J. Martin, K. Qiu, S.A. Shevlin, A.D. Handoko, X. Chen, Z. Guo, J. Tang, Angew. Chem. Int. Ed. 53 (2014) 9240–9245.
- [15] C. Bianchi, F. Porta, L. Prati, M. Rossi, Top. Catal. 13 (2000) 231–236.
- [16] C.-J. Liu, Nanoscale Res. Lett. 5 (2010) 124–129.
- [17] X. Huang, M.A. El-Sayed, J. Adv. Res. 1 (2010) 13–28.
- [18] M. Bowker, P.R. Davies, L.S. Al-Mazroai, Catal. Lett. 128 (2009) 253–255.
- [19] Z.H.N. Al-Azri, W.-T. Chen, A. Chan, V. Jovic, T. Ina, H. Idriss, G.I.N. Waterhouse, J. Catal. 329 (2015) 355–367.
- [20] F. Porta, L. Prati, M. Rossi, S. Coluccia, G. Martra, Catal. Today 61 (2000) 165–172.
- [21] M. Murdoch, G.I.N. Waterhouse, M.A. Nadeem, J.B. Metson, M.A. Keane, R.F. Howe, J. Llorca, H. Idriss, Nat. Chem. 3 (2011) 489–492.
- [22] Z. Zhang, G. Mestl, H. Knozinger, W.M.H. Sachtler, Appl. Catal. A-Gen. 89 (1992) 155–168.
- [23] A. Dickinson, D. James, N. Perkins, T. Cassidy, M. Bowker, J. Mol. Catal. A-Chem. 146 (1999) 211–221.
- [24] M. Yasuda, T. Tomo, S. Hirata, T. Shiragami, T. Matsumoto, Catalysts 4 (2014) 162.
- [25] X. Wang, K. Maeda, A. Thomas, K. Takanabe, G. Xin, J.M. Carlsson, K. Domen, M. Antonietti, Nat. Mater. 8 (2009) 76–80.
- [26] G.G. Zhang, J.S. Zhang, M.W. Zhang, X.C. Wang, J. Mater. Chem. 22 (2012) 8083–8091.
- [27] J.-D. Grunwaldt, C. Kiener, C. Wögerbauer, A. Baiker, J. Catal. 181 (1999) 223–232.
- [28] F.X. Zhang, J.X. Chen, X. Zhang, W.L. Gao, R.C. Jin, N.J. Guan, Catal. Today 93–95 (2004) 645–650.
- [29] P. Wu, J. Wang, J. Zhao, L. Guo, F.E. Osterloh, Chem. Commun. 50 (2014) 15521–15524.
- [30] X. Li, G. Hartley, A.J. Ward, P.A. Young, A.F. Masters, T. Maschmeyer, J. Phys. Chem. C 119 (2015) 14938–14946.